Design of a Novel High-Reliability Step-up DC-DC Converter with ZCS Characteristics

Seyed Reza Mosayyebi*[1],Mojtaba Ajoudani[2], Ramazan TeimouriYansari[3]

Abstract– In many applications such as photovoltaic (PV) farms, high-reliability step-up DC-DC converters have gained increasing attention. One of the issues with the power converter is the reliability problem. The high-step converters with lower-power semiconductors are more reliable. This article introduces a novel step-up DC-DC converter with zero current switching (ZCS) for semiconductor equipment. The suggested converter has only one switch and therefore is more reliable. The performance of the traditional converter and the suggested one has been investigated in the MATLAB/Simulink environment. The simulation results show that the suggested converter has a higher gain than the traditional one and when employed in a PV system, it injects more power into the network, indicating its superiority. At the same time, under similar variations in radiation and to reach the maximum power point, the suggested converter's duty cycle changes less, which shows its more suitable performance.

Keywords: Photovoltaic (PV), Reliability, High Step converters, Zero Current Switching (ZCS)

1. Introduction

In recent decades, energy security has become a major issue. Fossil fuels are running out, and all countries have aimed to decrease their dependence on fossil resources by implementing various planning. In developed countries, a terrifying idea has been created that if the use of renewable resources is not expanded, the day will come when there will be no energy sources at all [1].To meet the increasing demand for electrical energy in the face of problems caused by the depletion of conventional fossil resources, renewable energy sources have received more attention [2, 3].

The fossil energy scarcity and the increase in greenhouse gas emissions have led to the use of clean energy sources such as wind [4], and PV [5] systems. The output voltage of these sources is low, and they need voltage amplification to connect to the grid. If the active and passive components in a boost converter are ideal, the gain will be infinite as the duty cycle approaches one. The mentioned situation is not achievable in practical circuits. In traditional boost converters, if the duty cycle is increased, the high gain conversion will be achieved. However, this has led to the occurrence of electromagnetic interference (EMI) which adversely affects the performance of other systems [6, 7]. In actual conditions, due to the influence of parasitic elements, the voltage gain decreases as the duty cycle increases, especially when the duty cycle nears one. Due to the problems mentioned with conventional boost converters, it is necessary to introduce high-gain converters.

Many isolated converters have been suggested in various researches in which high-voltage gain can be achieved by increasing the conversion ratio in the high-frequency transformer. A full-bridge phase-shifting circuit was suggested in [8] that implements zero-voltage switching for a wide range of load utilizing the transformer leakage inductance. The high voltage stress over the output diode, low efficiency at high power cases, and the pulsating current are the main drawbacks of the mentioned converter. To increase the efficiency of the DC-DC converters and decrease their size, a non-isolated converter was employed to reach a voltage boost [9].

In high-power applications, the interleaving of several converters is usually utilized to enhance efficiency and reduce the volume of filter elements. So this method can be applied to boost voltage at high-power converters [10]. A three-level boost converter was introduced in [11]. This converter has low switching losses and low EMI levels. However, the static gain of this circuit is equal to that of a traditional boost one. When several traditional boost

1* **Corresponding Author**: Department of Electrical Engineering, Bandargaz Branch, Islamic Azad University, Bandargaz, Iran.
E-mail address: sr.mosayyebi@iau.ac.ir.

2Department of Electrical Engineering, Bandargaz Branch, Islamic Azad University, Bandargaz, Iran.

3Department of Computer Engineering, Bandargaz Branch, Islamic Azad University, Bandargaz, Iran.

Received: 2024.11.30; Accepted: 2024.12.31

circuits are cascaded [12], it results in a wide conversion ratio and reduced current ripple. To obtain a cascaded boost converter with only one switch, other switches can be replaced with corresponding diodes [13].A three-level quadratic boost circuit which has some advantages over the converter in [12, 13], was suggested in [14] to achieve high-voltage gain characteristics. There are two inductors in the structure of this converter, which makes the size and volume of the converter considerable for low-power applications. To increase the static gain of the converter in [13], a capacitor-inductor-diode unit is added to that converter. Significant conduction losses in low-power applications are a disadvantage of the converter proposed in [14].

Other types of high-gain boost converters employ coupled inductors as an alternative solution [15].A novel converter was suggested in [16], in which the turns ratio between the coils can be regulated to achieve extended static gain. A hybrid boost-flyback converter that combines some of the advantages of both flyback and conventional boost converters was suggested in [17]. However, the input current is high, so it must be reduced using an additional filter.

Capacitors as energy-storing devices, can be employed in DC-DC circuits to enhance the voltage gain, which are called boost circuits based on capacitor switching [18]. To achieve a voltage gain of two times that of a traditional boost circuit and decrease the voltage stress of the main switch, a novel boost circuit based on capacitor switching was suggested [19]. The proposed circuit is not suitable for high-current cases because the input inductance is large and the current of the switch has a non-negligible stress.

An interleaved boost converter employing a voltage doubler and an autotransformer with a turn ratio of one [20] to share the current between the branches. Using an auxiliary transformer which increases the cost, is the main drawback of this converter. Other boost converters are interleaved boost ones utilizing voltage multiplier cells that improve voltage gain. In this converter, the reverse-recovery currents flowing through the output diode and multiplier diodes are added together, so the efficiency may be decreased.

In this paper, a new high-gain DC-DC converter is presented. The suggested converter, due to the ZCS operation of the semiconductor elements, is more reliable. To describe the performance and application of the suggested converter, the organization of this paper is as follows: Section 2 describes the suggested converter and its modes. In Section 3, the implemented results confirm the paper's claim. In section 4, the proposed converter is utilized in a grid-connected PV array. Finally, conclusions are given in Section 5.

2. The suggested converter

The circuit configuration of the suggested converter is shown in Fig. 1. The inductance, the MOSFET, and the diode comprise one step-up conversion unit. The auxiliary circuit shunted with the main switch is formed by one capacitor and one inductance. The task of the auxiliary circuit is to increase the voltage gain of the converter. Due to the presence of this auxiliary circuit, the power switch and diode turn off and on at ZCS. The operation modes of the suggested converter are explained in the following description. For a simpler analysis of the circuit, the following assumptions are considered:

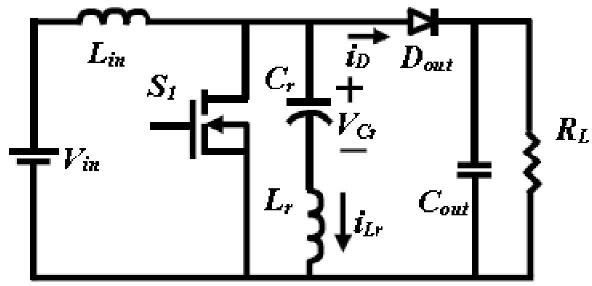

Fig. 1. The suggested high-gain DC-DC converter

1) All semiconductor types of equipment are ideal.
2) The output capacitor capacitance is large enough to minimize the output voltage variations.
3) A constant current source is assumed instead of the main inductor.

A) The operation mode

There are three commutation stages in each periodic operation of the suggested converter. The equivalent circuits for the three modes are depicted in Fig. 2.The converter works as follows:

Mode 1 [Fig. 2 (first circuit)]

At the beginning of this state, the power switch is off and the inductor current flowing through the switch completely commutates to the diode to feed the load. The auxiliary inductor current is also switched to the diode. The voltage across the auxiliary branch is V_0, so i_{Lr} increases sinusoidally, and the resonance capacitor charges. Therefore, the voltage of the resonant capacitor (V_{cr}) and the current of the resonant inductor (i_{Lr}) are computed as follows:

$$V_{cr}(t)=V_0-(V_0-V_{cr}(t_0))\cos(\omega_r t) -\sqrt{\frac{C_r}{L_r}}\,i_{Lr}(t_0)\sin(\omega_r t) \quad (1)$$

$$i_{Lr}(t)=\sqrt{\frac{C_r}{L_r}}(V_0+V_{cr}(t_0))\sin(\omega_r t) -i_{Lr}(t_0)\cos(\omega_r t) \quad (2)$$

Where $V_{cr}(t_0)$ is the voltage initial amount of the resonance capacitor at the beginning of this mode, $i_{Lr}(t_0)$ is the current initial amount of the resonance inductor, and $\omega_r=\frac{1}{2\pi\sqrt{L_r C_r}}$ .The current of i_{Lr} will reverse its direction. When i_{Lr} equals i_{in}, the first mode ends. Therefore, the diode can be turned off at ZCS. In this situation, the following relationships are established:

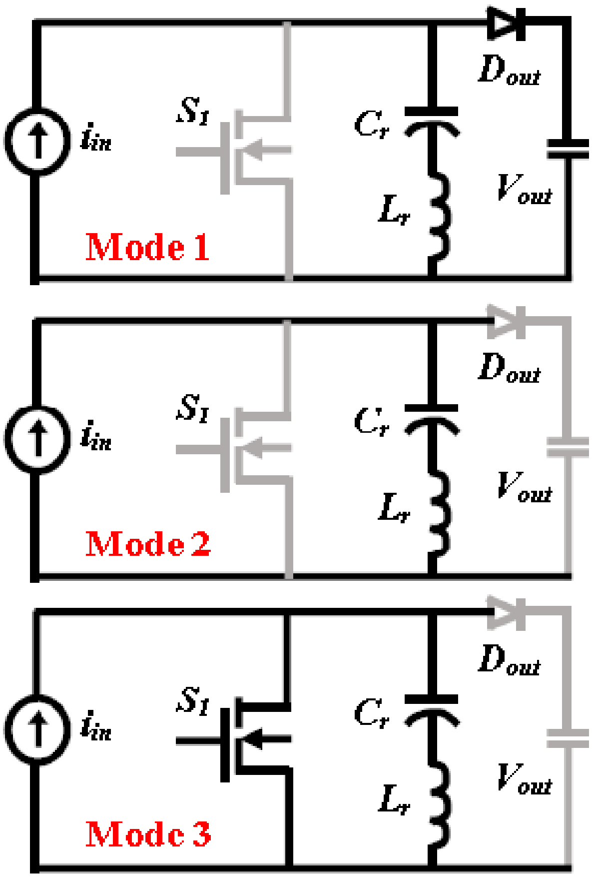

Fig. 2. The operating states and current paths in the converter

$$i_{in}(t)-i_{Lr}(t)=0 \quad (3)$$

$$i_{in}(t)=A\sin(\omega_r t)-B\cos(\omega_r t) \quad (4)$$

Where $A=\sqrt{\frac{C_r}{L_r}}(V_0+V_{cr}(t_0))$ and $B=i_{Lr}(t_0)$ .The duration time of this mode can be computed utilizing Eq. (5).

$$t_1=\frac{1}{\omega_r}\left(\sin^{-1}\left(\frac{i_{in}}{\sqrt{A^2+B^2}}\right)+\tan^{-1}\left(\frac{B}{A}\right)\right) \quad (5)$$

Mode 2 [Fig. 2 (the second circuit)]

This mode is started when the diode is turned off with a ZCS condition and the main inductor current flows to the auxiliary branch. The capacitor C_r is charging linearly to a positive amount. The equations for this case are as follows:

$$V_{cr}(t)=V_{cr}(t_1)+\frac{i_{in}t}{C_r} \quad (6)$$

$$i_{Lr}(t)=i_{in} \quad (7)$$

When the switch is turned on, this state ends and therefore, its duration is obtained according to Eq. (8).

$$t_2=T(1-D)-t_1 \quad (8)$$

Mode 3 [Fig. 2 (the third circuit)]

At the beginning of this mode, the firing pulse is applied to the switch. Since there is an auxiliary inductor in the circuit, the power switch turns on at ZCS situation. The auxiliary inductor and capacitor comprise a resonance mesh so the inductor current rises in sinusoidal form and the voltage of the capacitors decreases. The time domain equations of capacitor voltage and inductor current are given in Eqs. (9) and (10).

$$V_{cr}(t)=V_{cr}(t_2)\cos(\omega_r t)+\frac{i_{Lr}(t_2)}{C_r\omega_r}\sin(\omega_r t) \quad (9)$$

$$i_{cr}(t)=-C_r\omega_r V_{cr}(t_2)\sin(\omega_r t)+\frac{i_{Lr}(t_2)}{C_r\omega_r}\cos(\omega \quad (10)$$

Where $V_{cr}(t_2)$ is the voltage initial amount of the resonance capacitor at the beginning of this mode, $i_{Lr}(t_2)$ is the current initial amount of the resonance inductor.

B) The voltage gain

Fig. 3 is employed to obtain the voltage gain. According to this illustration, T is the switching period, and T_1 is the time duration of Mode 1.The voltage gain is obtained from Eqs. (11) to (15).

$$\frac{V_i}{L_{in}}DT=\frac{V_o-V_i}{L_{in}}t_1 \quad (11)$$

$$\frac{V_o}{V_i}=1+\frac{DT}{t_1} \quad (12)$$

$$\frac{V_o}{V_i} = 1 + \frac{\omega_r DT}{\sin^{-1}\left(\frac{i_{in}}{\sqrt{A^2+B^2}}\right) + \tan^{-1}\left(\frac{B}{A}\right)} \quad (13)$$

$$\frac{V_o}{V_i} = \frac{1}{1-D_{eff}} \quad (14)$$

$$\frac{1}{1-D_{eff}} = 1 + \frac{\omega_r DT}{\sin^{-1}\left(\frac{V_o}{D_{eff} R_L \sqrt{A^2+B^2}}\right) + \tan^{-1}(} \quad (15)$$

Where D_{eff} is the effective duty cycle, and R_L is the resistor of the load. If $t_l \geq (1-D)T$, the suggested structure operates as a traditional boost converter. The variation of current in various operating modes is depicted in Fig. 3.

C) The efficiency

A simple yet critical ratio determines the efficiency of DC-DC converters: the value of output power divided by the input power. This ratio is often explained as a percentage as follows:

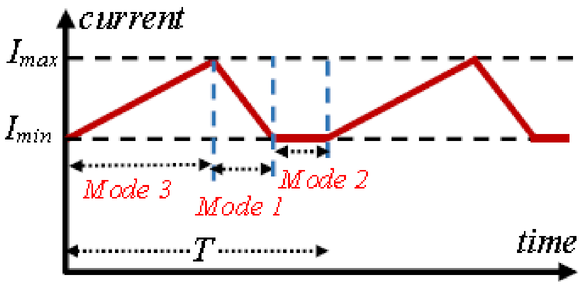

Fig. 3. Current changes in various operating modes

$$\eta\% = \frac{P_{out}}{P_{in}} \times 100 = \frac{V_{out}\, i_{out}}{V_{in}\, i_{in}} \times 100 \quad (16)$$

Where η is the efficiency, P_{out} is the output power, P_{in} is the input power, V_{out} is the output voltage, V_{in} is the input voltage, i_{out} is the output current, and i_{in} is the input current.

3. Results of the simulation

In this section, a simulation circuit is implemented to verify the claims. The circuit parameters are listed in Table 1. Figs. (4)-(7) illustrate the simulated waveforms for the suggested converter. As seen in Fig. 4, the diode turns off under the ZCS situation. The high-frequency components, as seen in this figure, are related to the charging and discharging of the parasitic capacitor. When the gate signal is ordered, the current of the power switch is zero, i.e., the power switch turns on under the ZCS situation, as shown in Fig. 5.When the power switch and output diode are off, the main inductance current equals the auxiliary inductance, as depicted in Fig. 6.When the major inductance current flows to the auxiliary branch, the capacitor C_r is charging linearly to a higher positive amount .If the power switch conducts, the auxiliary inductor and capacitor will comprise a resonance mesh and so the inductor current will rise in sinusoidal form and the voltage of the capacitors will decrease. This operation can be seen in Fig. 7.

To compare the voltage gain of the suggested converter with a conventional one, the voltage gain of these two converters is plotted versus duty cycle variations, as depicted in Fig. 8. It is observed that the suggested converter has a higher voltage gain than the conventional one, which shows its superiority.

Table 1. Circuit parameters

Parameter	Value
Main inductors	**600 µH**
Output Capacitor	**10 µF**
Resonance Capacitor	**370 nF**
Resonance Inductor	**50 µH**
Switching Frequency	**50 kHz**
Input Voltage	**10 V**

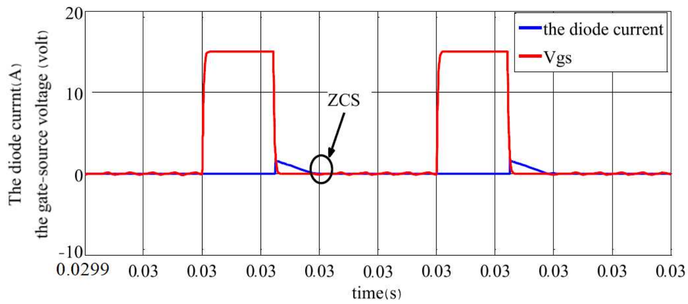

Fig. 4. The current of the diode and gate driving signal

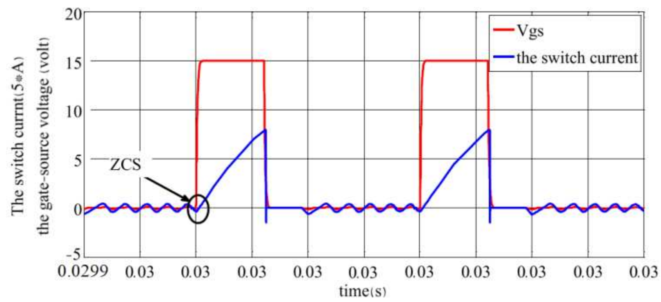

Fig. 5. The current of the power switch and gate driving signal

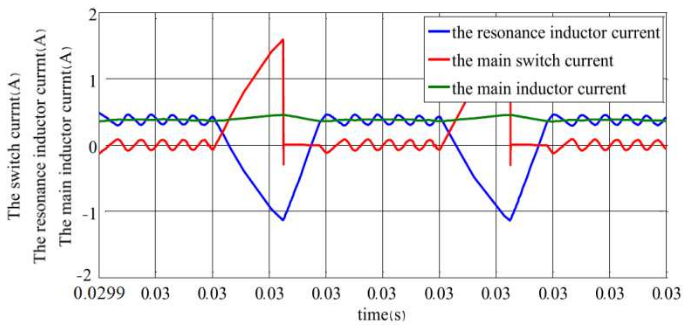

Fig. 6. The current of the power switch, resonance inductance, and input inductance

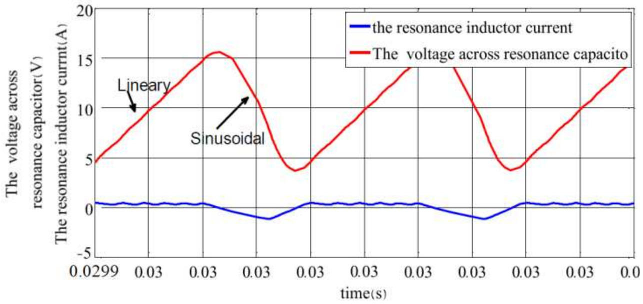

Fig. 7. The voltage of the power switch, and the current of the input inductor

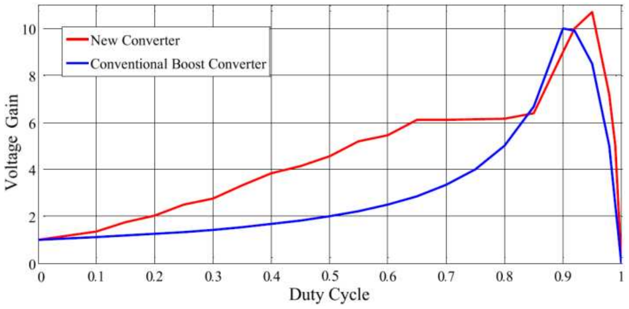

Fig. 8. The voltage gain of the conventional and suggested converter

4. Application of suggested converter

In this section, the suggested converter is employed in a PV (SunPower SPR-305) system that injects power into a grid. As depicted in Figure 9, with the change in irradiance, the PV array's output current, power, and voltage change, in which case the maximum power point tracking (MPPT) system must play its role properly. If the radiation is increased, according to the use of MPPT, the voltage increases slightly and in this condition, the current increases more. It is assumed that the radiation profile of the studied site for the PV module has a profile seen in Fig. 10.This radiation profile is the same for the two operating conditions, namely the photovoltaic system with the conventional boost converter and with the suggested converter. The block diagram of the grid-connected PV system is depicted in Fig. 11.In this structure, a traditional boost converter is first employed. The duty cycle variations are made using MPPT to capture maximum energy and transfer it to the grid. Fig. 12 and Fig. 13 show the variations of the duty cycle and the transmitted power to the grid, respectively.

In the second step, the suggested converter is employed to track the optimum point of the photovoltaic arrays. The duty cycle variations and the transmitted power to the grid, when the suggested converter is employed, are depicted in Fig.14 and Fig. 15 respectively. From Fig. 13 and Fig. 15, it is clear that a higher power can be transmitted to the grid. Therefore, the suggested converter can improve the MPPT tracking for PV systems. Since the diode is turned off under ZCS situation, the diode losses can be low and therefore the diode failure rate is reduced, making the converter more reliable. On the other hand, one power switch is essential, which makes the converter easy to control. The easy control system can enhance the reliability of the converter.

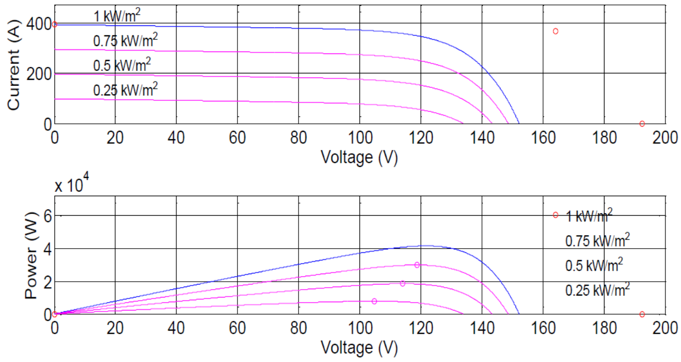

Fig. 9. The simulated characteristics of the PV module

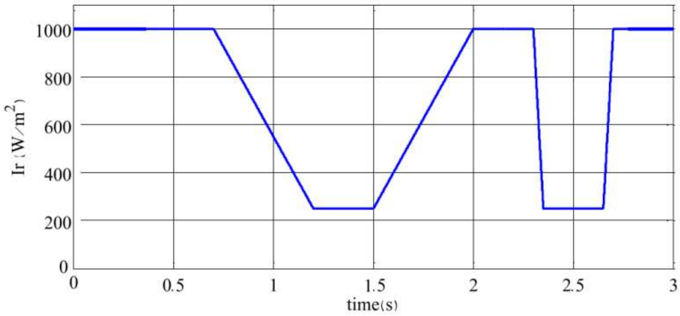

Fig. 10. The irradiance profile at the selected site

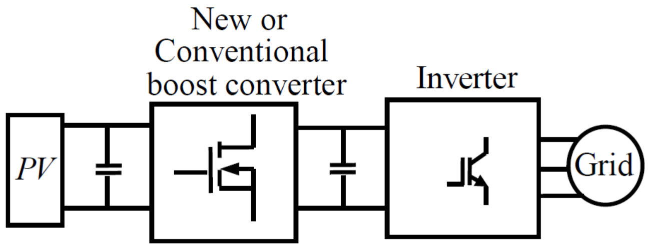

Fig. 11. The overall topology of the network-connected photovoltaic system

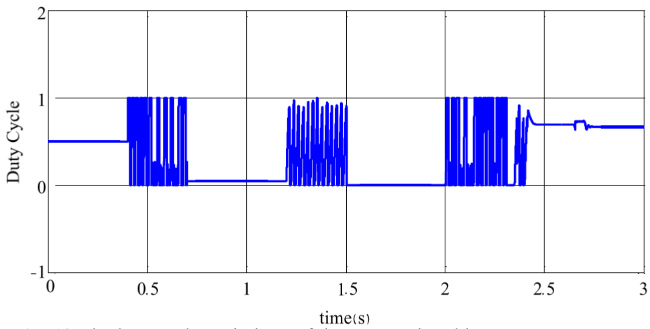

Fig. 12. Theduty cycle variations of the conventional boost structure

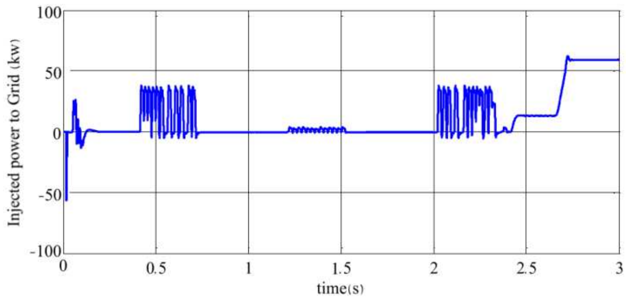

Fig. 13. The injected power from photovoltaic to the network under the

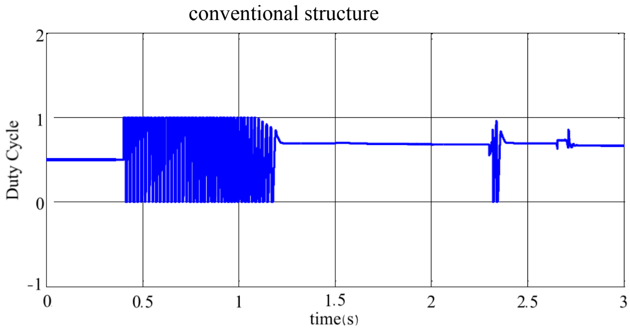

Fig. 14. Theduty cycle variations of the suggested boost structure

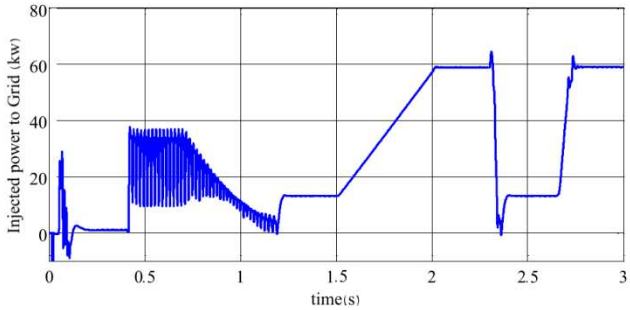

Fig. 15. The injected power from photovoltaic to the network under the suggested structure

The efficiency of the conventional converter and the suggested converter in terms of power was shown in Fig. 16. It is observed that the suggested converter has a higher efficiency, which indicates more power injection into the network.

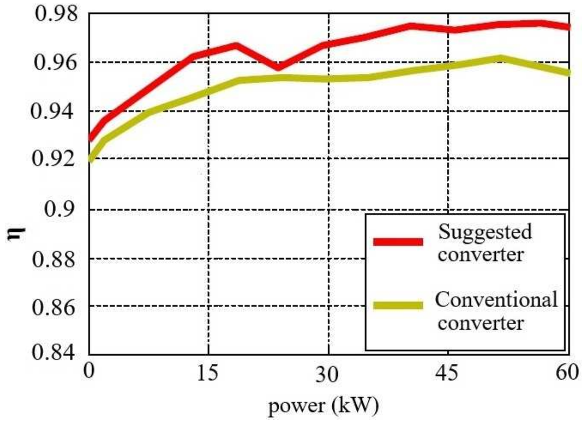

Fig. 16. Efficiency vs power

5. Conclusions and future trends

This article has analyzed and simulated a new high-gain DC-DC converter. It is shown that the main power switch exhibits ZCS commutation and the diode can be turned off under ZCS condition. The analytical analysis and the simulation results have confirmed the claims. Since the diode can be turned off under the ZCS situation, the failure rate of the diode will be at a low level. This shows the superiority of the suggested converter over the traditional one and makes it more reliable. The simulation results indicate that the voltage gain of the suggested converter is higher and it injects more power into the grid. This indicates a higher efficiency of the suggested converter compared to the traditional one.

In the future, we would like to investigate different reliability prediction models for the traditional and suggested converters.

Conflict of interest

The article's authors declare that this research has no conflict of interest.

References

[1] J.A. Pec as Lopes , N. Hatziargyriou , J. Mutale , P. Djapic , N. Jenkins, “Integrating distributed generation into electric power systems A review of drivers, challenges and opportunities,” Electric Power Systems Research, vol.77, pp. 1189–1203, 2007.

[2] F. Blaabjerg, F. Iov, T. Kerekes, and R. Teodorescu, “Trends in power electronics and control of renewable energy systems”, 14th Int. Power Electronics and Motion Control Conf. (EPE/PEMC) 1, K-1–K-19, 2010.

[3] EPIA, “Global market outlook for photovoltaics until 2013”, Eur. Photovoltaic Industry Association 1, CD-ROM , 2010.

[4] Kesraoui M, Korichi N, Belkadi A, “ Maximum power point tracker of wind energy conversion system,” Renew Energy, vol. 36, pp. 2655- 2662, 2011.

[5] Shuhui L, Timothy AH, Dawen L, Fei H, “ Integrating photovoltaic and power converter characteristics for energy extraction study of solar PV systems,” Renew Energy, vol.36, pp. 3238-3245, 2011.

[6] Rahimi, T.; Hosseini, S.H., “EMI consideration of high reliability electrical power subsystem (EPS) of satellite”, in 6th Power Electronics, Drives Systems & Technologies Conference (PEDSTC) , Tehran, Iran, pp. 412 - 417 , 2015.

[7] Rahimi, T., YousefiKhangah, S., &Yousefi, B, “ Reduction EMI due to di/dt and dv/dt DC and AC Sides of BLDC Motor Drive”, In 5th Power Electronics, Drive Systems and Technologies Conference (PEDSTC); 5-6 Feb., Tehran, Iran, pp. 428-433, 2014.

[8] Chen, Z., Liu, S., Shi, L, “A soft switching full bridge converter with reduced parasitic oscillation in a wide load range”, IEEE Trans. Power Electron., vol. 29, pp. 801–812, 2014.

[9] Hu, X., Gong, C, “A high voltage gain dc–dc converter integrating coupled-inductor and diode–capacitor techniques”, IEEE Trans. Power Electron., vol. 29, pp. 789–800, 2014.

[10] Garth, D.R., Muldoon, W.J., Benson, G.C., Costague, E.N, “Multi-phase, 2-kilowatt, high-voltage, regulated power supply”, Proc. IEEE Power Conditioning Specialists Conf., pp. 110–116, 1971.

[11] Lin, B.-R., Hsin-Hung, L., Yei-Lang, H., “Single-phase power factor correction circuit with three-level boost converter”, Proc. IEEE Int. Symp. on Industrial Electronics, pp. 445–45, 1999.

[12] Huber, L., Jovanovic, M.M., “A design approach for server

power supplies for networking applications", Proc. IEEE Applied Power Electronics Conf. and Exposition, pp. 1163–116, 2000.

[13] Xiaogang, F., Jinjun, L., Lee, F.C. , "Impedance specifications for stable dc distributed power systems", IEEE Trans. Power Electron., vol. 17, pp. 157–162 , 2002.

[14] Yang, P., Xu, J., Zhou, G., Zhang, S. , " A new quadratic boost converter with high voltage step-up ratio and reduced voltage stress", Proc. IEEE Seventh Int. Power Electronics and Motion Control Conf., pp. 1164–1168, 2012.

[15] Himmelstoss, F.A., Wurm, P.H., " Low-loss converters with high step-up conversion ratio working at the border between continuous and discontinuous mode", Proc. IEEE Int. Conf. on Electronics, Circuits and Systems, pp. 734–737, 2000.

[16] Zhao, Q., Lee, F.C., " High-efficiency, high step-up dc–dc converters', IEEE Trans.Power Electron. ", vol. 18, pp. 65–73, 2003.

[17] Tseng, K.C., Liang, T.J., " Novel high-efficiency step-up converter", IEE Proc., Electr. Power Appl., vol.151, pp. 182–190, 2004.

[18] Liang, T.-J., Chen, S.-M., Yang, L.-S., Chen, J.-F., Ioinovici, A., " Ultra-large gain step-up switched-capacitor dc-dc converter with coupled inductor for alternative sources of energy", IEEE Trans. Circuits Syst. I, Regul. Pap., vol.59, pp. 864–874, 2012.

[19] Rosas-Caro, J.C., Ramirez, J.M., Peng, F.Z., Valderrabano, A., " A dc-dc multilevel boost converter', IET Power Electron. ", vol. 3, pp. 129–137, 2010.

[20] Yungtaek, J., Jovanovic, M.M., " New two-inductor boost converter with auxiliary transformer ", IEEE Trans. Power Electron., vol. 19, pp. 169–175, 2004.